Kinetic and Density Functional Studies on Alkyl-Carbene Elimination from Pd^{II} Heterocylic Carbene Complexes: A New Type of Reductive Elimination with Clear Implications for Catalysis

David S. McGuinness,[†] Nadja Saendig,[‡] Brian F. Yates,*[,†] and Kingsley J. Cavell*[,†,§]

Contribution from the School of Chemistry, University of Tasmania, GPO Box 252-75 Hobart, Tasmania 7001, Australia, and Institut für Organische Chemie, Technische Universität Berlin, Strasse des 17. Juni 135, D-10623 Berlin, Germany

Received November 2, 2000

Abstract: A number of new methyl−Pd^{II} complexes of heterocyclic carbenes of the form $[PdMe(tmiy)L_2]BF_4$ have been prepared, and their reaction behavior has been studied (tmiy = 1,3,4,5-tetramethylimidazolin-2-ylidene, L = cyclooctadiene (**8**), methyldiphenylphosphine (**9**), triphenyl phosphite (**10**), triphenylphosphine (**11**)). In common with other hydrocarbyl−M carbene complexes (M = Pd, Ni) the complexes are predisposed to a facile decomposition process. A detailed mechanism for the process and of the decomposition pathway followed is presented herein. All complexes decompose with first-order kinetics to yield 1,2,3,4,5-pentamethylimidazolium tetrafluoroborate and Pd^0 species. The kinetic investigations combined with density functional studies show that the complexes decompose via a mechanism of concerted reductive elimination of the methyl group and carbene. The reaction represents a new type of reductive elimination from transition metals and also represents a low-energy pathway to catalyst deactivation for catalysts based on heterocyclic carbenes. The theoretical studies indicate extensive involvement of the p(π) orbital on the carbene carbon in the transition structure. Methods of stabilizing catalysts based on heterocyclic carbene complexes are suggested, and the possibility of involvement of carbene species during catalysis in ionic liquids is discussed.

1. Introduction

One of the most active areas of research in chemistry is the search for new homogeneous catalysts for organic transformations. Frequently, this involves the preparation and application of new ancillary ligands to influence the properties of metal-based catalysts.[1] In recent years there has been much interest in the application of heterocyclic carbenes as ancillary ligands in various transition metal-catalyzed reactions; these include furan synthesis (Ru),[2] olefin metathesis (Ru),[3−8] hydrosilylation (Rh),[9−13] copolymerization (Pd),[14] and Heck-type coupling reactions (Pd, Ni).[15−23] The role of the carbene is thought to be similar to that of the ubiquitous tertiary phosphine ligands, although it is thought that the carbenes are stronger donors than even the highly basic phosphines such as PMe_3 and PCy_3.[17,20,24−28] Hence, the reversible dissociation that is a characteristic of the phosphines probably does not occur for heterocyclic carbenes.

A common problem encountered with phosphine-based catalysts is decomposition resulting from P−C bond cleavage.[29]

[†] University of Tasmania.
[‡] Technische Universität Berlin.
[§] Present address: Department of Chemistry, Cardiff University, PO Box 912, Cardiff, CF1 3TB, UK. E-mail: cavellkj@cf.ac.uk.

(1) Herrmann, W. A.; Cornils, B. *Angew. Chem., Int. Ed. Engl.* **1997**, *36*, 1048.
(2) Kücükbay, H.; Cetinkaya, B.; Salaheddine, G.; Dixneuf, P. H. *Organometallics* **1996**, *15*, 2434.
(3) Weskamp, T.; Schattenmann, W. C.; Spiegler, M.; Herrmann, W. A. *Angew. Chem., Int. Ed.* **1998**, *37*, 2490.
(4) Weskamp, T.; Kohl, F. J.; Hieringer, W.; Gleich, D.; Herrmann, W. A. *Angew. Chem., Int. Ed.* **1999**, *38*, 2146.
(5) Ackermann, L.; Fürstner, A.; Weskamp, T.; Kohl, F. J.; Herrmann, W. A. *Tetrahedron Lett.* **1999**, *40*, 4787.
(6) Huang, J.; Stevens, E. D.; Nolan, S. P.; Petersen, J. L. *J. Am. Chem. Soc.* **1999**, *121*, 2674.
(7) Huang, J.; Schanz, H.-J.; Stevens, E. D.; Nolan, S. P. *Organometallics* **1999**, *18*, 5375.
(8) Jafarpour, L.; Schanz, H.-J.; Stevens, E. D.; Nolan, S. P. *Organometallics* **1999**, *18*, 5416.
(9) Hill, J. E.; Nile, T. A. *J. Organomet. Chem.* **1977**, *137*, 293.
(10) Lappert, M. F.; Maskell, R. K. *J. Organomet. Chem.* **1984**, *264*, 217.
(11) Herrmann, W. A.; Goossen, L. J.; Köcher, C.; Artus, G. R. J. *Angew. Chem., Int. Ed. Engl.* **1996**, *35*, 2805.
(12) Enders, D.; Gielen, H.; Breuer, K. *Tetrahedron: Asymmetry* **1997**, *8*, 3571.
(13) Enders, D.; Gielen, H.; Runsink, J.; Breuer, K.; Brode, S.; Boehn, K. *Eur. J. Inorg. Chem.* **1998**, 913.
(14) Gardiner, M. G.; Herrmann, W. A.; Reisinger, C.-P.; Schwarz, J.; Spiegler, M. *J. Organomet. Chem.* **1999**, *572*, 239.
(15) Herrmann, W. A.; Elison, M.; Fischer, J.; Köcher, C.; Artus, G. R. J. *Angew. Chem., Int. Ed. Engl.* **1995**, *34*, 2371.
(16) Herrmann, W. A.; Reisinger, C.-P.; Spiegler, M. *J. Organomet. Chem.* **1998**, *557*, 93.
(17) Schwarz, J.; Böhm, V. P. W.; Gardiner, M. G.; Grosche, M.; Hermann, W. A.; Hieringer, W.; Raudaschl-Sieber, G. *Chem. Eur. J.* **2000**, *6*, 1773.
(18) Enders, D.; Gielen, H.; Raabe, G.; Runsink, J.; Teles, J. H. *Chem. Ber.* **1996**, *129*, 1483.
(19) McGuinness, D. S.; Green, M. J.; Cavell, K. J.; Skelton, B. W.; White, A. H. *J. Organomet. Chem.* **1998**, *565*, 165.
(20) McGuinness, D. S.; Cavell, K. J.; Skelton, B. W.; White, A. H. *Organometallics* **1999**, *18*, 1596.
(21) McGuinness, D. S.; Cavell, K. J. *Organometallics* **2000**, *19*, 741.
(22) Zhang, C.; Huang, J.; Trudell, M. L.; Nolan, S. P. *J. Org. Chem.* **1999**, *64*, 3804.
(23) Caló, V.; Del Sole, R.; Nacci, A.; Schingaro, E.; Scordari, F. *Eur. J. Org. Chem.* **2000**, 869.
(24) Lappert, M. F. *J. Organomet. Chem.* **1975**, *100*, 139.
(25) Lappert, M. F.; Pye, P. L. *J. C. S. Dalton* **1977**, 2172.
(26) Lappert, M. F. *J. Organomet. Chem.* **1988**, *358*, 185.
(27) Öfele, K.; Herrmann, W. A.; Mihalios, D.; Elison, M.; Herdtweck, E.; Scherer, W.; Mink, J. *J. Organomet. Chem.* **1993**, *459*, 177.
(28) Huang, J.; Schanz, H.-J.; Stevens, E. D.; Nolan, S. P. *Organometallics* **1999**, *18*, 2370.

10.1021/ja003861g CCC: $20.00
Published on Web 04/06/2001

Accordingly, it is often necessary to use a large excess of the ligand relative to the metal in catalyst formulations. In contrast, one of the reasons for the success of heterocyclic carbenes in catalysis is thought to be the high stability of the subsequent complexes, which results from the strength of the M−carbene bond. However, we have previously discovered a facile mode by which the M−carbene bond in Pd complexes may be broken, leading to decomposition.[19,20,30] In particular, decomposition is observed when the Pd complexes also contain a hydrocarbyl group, and the process is characterized by the elimination of a hydrocarbylimidazolium salt and M^0 species (Reaction 1). This presents a potentially serious drawback in the application of complexes of heterocyclic carbenes in catalysis reactions involving hydrocarbon substrates.

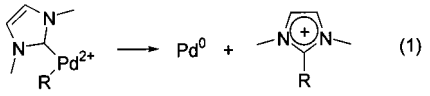

The decomposition reaction was first observed when the thermal behavior of [PdMe(dmiy)(cod)]BF_4 (**1**) was monitored (dmiy = 1,3-dimethylimidazolin-2-ylidene).[19] Unexpectedly, it was found that the cod ligand simply dissociates during decomposition, and the sole products of the reaction are 1,2,3-trimethylimidazolium tetrafluoroborate and Pd^0 (Reaction 2).

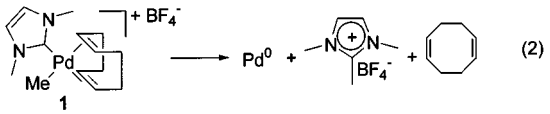

In subsequent mechanistic studies on the Heck reaction we found that neutral aryl Pd^{II} complexes **2** and **3** are also prone to decompose via elimination of imidazolium salts (Reaction 3).[20]

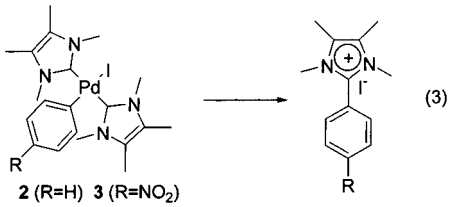

Moreover, it was found that halide abstraction from **3**, to give a cationic complex, resulted in a much higher rate of decomposition when compared to the neutral complex. Ensuing studies into the Heck reaction showed that at lower temperatures the reaction is competitive with β-hydride elimination; halide abstraction from **3** in the presence of *n*-butylacrylate gave both the imidazolium salt **4** and cinnamate **5**, presumably through insertion intermediate **6** (Scheme 1). Significantly, the elimination reaction has also been observed for the Ni^{II} complex Ni(Me)(tmiy)$_2$I (**7**, tmiy = 1,3,4,5-tetramethylimidazolin-2-ylidene), which could not be isolated pure because of the ease at which it eliminated the pentamethylimidazolium cation even at −40 °C (Reaction 4).[20]

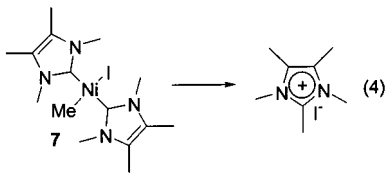

Furthermore,we have recently reported the elimination of an acyl-imidazolium salt from Pd during carbonylation studies of a Me−Pd carbene complex.[30]

Scheme 1

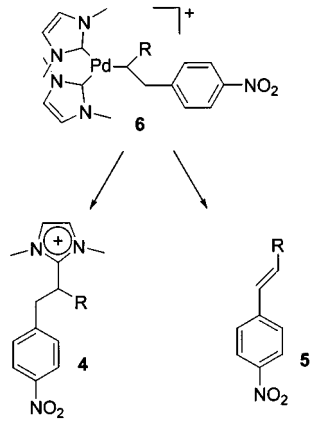

Scheme 2. Possible Mechanisms for Elimination of Alkyl-imidazolium Salts from Pd−Carbene Complexes

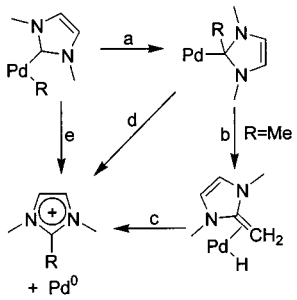

Several mechanisms by which this mode of decomposition occurs may be envisaged (Scheme 2). For example, migratory insertion of the carbene into the Pd−R bond (path a) would give a complex in which the carbene ligand has (formally) become an anionic alkyl ligand. Examples of migration of Fischer and Schrock carbenes into both alkyl− and hydride−metal bonds are common.[31−41] Furthermore, the carbene moiety is isoelectronic with isocyanide, for which insertion into the Pd−Me bond is known.[42] In the case of R being an alkyl group the next step in decomposition could involve β-hydride elimination to give a complex containing a coordinated enediamine fragment and a hydride ligand (path b). From this complex reductive elimination of H^+, aided by the basic enediamine ligand,[43] would give the imidazolium salt and Pd^0 (path c). When R is an aryl or acyl group, then a pathway involving β-hydride elimination is not available. In this case (and also possibly in

(29) Garrou, P. E. *Chem. Rev.* **1985**, *85*, 171.
(30) McGuinness, D. S.; Cavell, K. J. *Organometallics* **2000**, *19*, 4918.
(31) Threlkel, R. S.; Bercaw, J. E. *J. Am. Chem. Soc.* **1981**, *103*, 2650.
(32) Jernakoff, P.; Cooper, N. J. *J. Am. Chem. Soc.* **1984**, *106*, 3026.
(33) Green, J. C.; Green, M. L. H.; Morley, C. P. *Organometallics* **1985**, *4*, 1302.
(34) Osborn, V. A.; Parker, C. A.; Winter, M. J. *J. Chem. Soc., Chem. Commun.* **1986**, 1185.
(35) Ziegler, T.; Versluis, L.; Vincenzo, T. *J. Am. Chem. Soc.* **1986**, *108*, 612.
(36) Carter, E. A.; Goddard, W. A., III. *J. Am. Chem. Soc.* **1987**, *109*, 579.
(37) Carter, E. A.; Goddard, W. A., III. *Organometallics* **1988**, *7*, 675.
(38) Winter, M. J. *Polyhedron* **1989**, *8*, 1583.
(39) Winter, M. J.; Woodward, S. *J. Organomet. Chem.* **1989**, *361*, C18.
(40) Davey, C. E.; Devonshire, R.; Winter, M. J. *Polyhedron* **1989**, *8*, 1863.
(41) Fischer, H.; Jungklaus, H. *J. Organomet. Chem.* **1999**, *572*, 105.
(42) Yamamoto, Y.; Yamazaki, H. *Bull. Chem. Soc. Jpn.* **1970**, *43*, 3.
(43) Kuhn, N.; Bohnen, H.; Henkel, G.; Kreutzberg, J. *Z. Naturforsch.* **1996**, *51 b*, 1267.

the case where R = alkyl group) reductive elimination of the alkyl ligand that results from the initial insertion would yield the observed decomposition products (path d).

N-heterocylic carbenes bind with metals in a manner different to that observed for Fischer and Schrock carbenes. As a consequence of electron density donated from the two N atoms, heterocyclic carbenes act as pure σ-donors, with little if any of the π-back-bonding that occurs in other classes of carbene complexes.[44,45] Consistent with this view, $M-C_{carbene}$ bond lengths for heterocyclic carbenes lie in the range for normal $M-C(sp^3/sp^2)$ single bonds.[15,20] In light of this observation it would seem not unreasonable that the $M-C_{carbene}$ bond could show aspects of chemical reactivity similar to other M−C single bonds. Thus, the decomposition of alkyl, aryl, or acyl Pd carbene complexes could arguably occur via a concerted reductive elimination to yield in one step the imidazolium ion and Pd^0 (path e) in an analogous manner to the well-known reductive elimination of R−R′ and R−X from transition metals.[46,47]

One of the most important goals of a catalyst design study is to understand the mechanism by which the catalytic reaction occurs, allowing a logical approach to the design process. Likewise, understanding how an active catalyst is deactivated may allow the deactivation process to be controlled. The decomposition reaction we have described above appears to be a common mode of carbene loss for hydrocarbyl−carbene complexes and indicates a significant pathway for catalyst deactivation. Hydrocarbyl species are expected to be intermediates in many catalytic reactions including those carried out with transition metal−carbene complexes (for example Heck-type coupling,[15−23] ethylene-CO copolymerization[14] and ethylene polymerization[48,49]). It was thus of considerable interest to us to elucidate the detailed mechanism for the reaction such that steps can be taken to limit its occurrence. We report here further details of the reaction together with combined kinetic and theoretical studies aimed at deducing the mechanism of the reaction.

2. Results and Discussion

2.1. Synthesis. To study the kinetics of the decompositon reaction a number of complexes (**8**−**11**) were prepared via halide abstraction from the dimer $[PdMeCl(tmiy)]_2$[19] in the presence of coordinating ligands (Scheme 3). Complexes have been characterized by ^{1}H-, ^{13}C-, and ^{31}P NMR spectroscopy, mass spectroscopy and elemental analysis with the exception of **11**, the instability of which prevented elemental analysis. Consequently, a high-resolution MS has been obtained for **11**.

A *cis* carbene/methyl group arrangement for complexes **9**−**11** is expected from the relative *trans* influences of the carbene versus the phosphite/phosphine, the carbene being a stronger σ-donor than the phosphorus ligands. The ^{31}P spectra of **9**−**11** confirm this viewpoint. The ^{31}P NMR spectrum of complex **10** contains two doublets at 120.3 and 113.4 ppm with a P−P coupling constant of 72 Hz, showing the inequivalence of each phosphite ligand. Complex **11** shows two doublets at 34.2 and 21.4 ppm (J = 30 Hz), and complex **9**, two doublets at 12.3 and 0.8 ppm (J = 33 Hz). Complexes **10** and **11** could also be prepared via addition of 2 equiv of the appropriate phosphorus ligand to **8**. ^{1}H NMR spectroscopy showed the clean formation of the phosphite/phosphine complex along with free cyclooctadiene.

Scheme 3. Synthesis of Me−Pd Carbene Complexes[a]

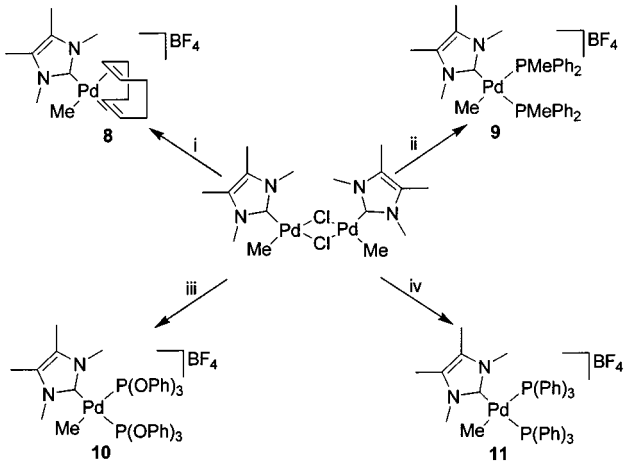

[a] i) $AgBF_4$, cod; ii) $AgBF_4$, 2 $PMePh_2$; iii) $AgBF_4$, 2 $P(OPh)_3$; iv) $AgBF_4$, 2 $P(Ph)_3$.

2.2. Kinetic Studies. On warming, complexes **8**−**11** were found to decompose cleanly to the 1,2,3,4,5-pentamethyl imidazolium ion with rates measurable by ^{1}H NMR. The imidazolium cation exhibits signals at 3.64, 2.62, and 2.21 ppm for the $N-CH_3$, C_2-CH_3, and backbone CH_3 protons, respectively. During the decomposition of complexes **9**−**11**, bis(phosphite/phosphine) Pd^0 complexes, $Pd(PMePh_2)_2$, $Pd[P(OPh)_3]$, and $Pd(PPh_3)_2$,[50] form initially and then slowly decompose to give Pd deposits (Reaction 5).

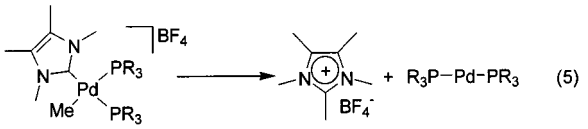

The ^{1}H NMR spectrum of decomposing **10** shows the formation of pentamethylimdazolium accompanied by extra signals at 6.7−7.2 ppm, arising from the formation of $Pd[P(OPh)_3]_2$. In the ^{31}P NMR spectrum of **10** the two doublets are replaced by a singlet at 141.0 ppm, due to $Pd[P(OPh)_3]_2$. For complex **11** these extra peaks appear at 7.60−7.85 ppm in the ^{1}H NMR spectrum and as a singlet a 35.4 ppm in the ^{31}P spectrum, resulting from $Pd(PPh_3)_2$. Complex **8** decomposes to give metallic Pd and free cyclooctadiene.

The rates of decomposition of **8**−**11** were obtained by monitoring the disappearance of the $N-CH_3$ or $C-CH_3$ signals in the ^{1}H NMR spectrum at 20 °C. In all cases linear first-order rate plots were obtained (Table 1). Rate constants were also measured for the decomposition of **10** and **11** in the presence of 1 equiv of COD. This was achieved by adding 2 equiv of the respective phosphorus ligand to an NMR solution of **8**. Table 1 shows that the rates of decomposition followed the order: complex **9** < **8** < **10** < **11**. The presence of 1 equiv of COD slows the decomposition of complex **11** somewhat.

Attempts to make the tricyclohexylphosphine (PCy_3) analogue **12** using the same technique failed. NMR studies of the product solution showed that it contained pentamethylimidazolium

(44) Fröhlich, N.; Pidun, U.; Stahl, M.; Frenking, G. *Organometallics* **1997**, *16*, 442.
(45) Boehme, C.; Frenking, G. *Organometallics* **1998**, *17*, 5801.
(46) Stille, J. K. In *The Chemistry of the Metal Carbon Bond*; Hartley, F. R., Patai, S., Eds.; Wiley-Interscience, 1985; Vol. 2, p 742.
(47) Collman, J. P.; Hegedus, L. S.; Norton, J. R.; Finke, R. G. *Principles and Applications of Organotransition Metal Chemistry*; University Science Books: Mill Valley, CA, 1987.
(48) Döhring, A.; Göhre, J.; Jolly, P. W.; Kryger, B.; Rust, J.; Verhovnik, G. P. J. *Organometallics* **2000**, *19*, 388.
(49) McGuinness, D. S.; Cavell, K. J. Unpublished results.
(50) Urata, H.; Suzuki, H.; Moro-oka, Y.; Ikawa, T. *J. Organomet. Chem.* **1989**, *364*, 235.

Table 1. Decomposition Kinetics for Complexes **8**−**12**

complex	$k/10^{-4}$ s^{-1} [a]	$t_{1/2}/10^3$ s	θ (deg)[b]	pK_a[b]
8	0.71 ± 0.03 (0.995)	9.8		
9	0.518 ± 0.009 (0.998)	13.4	136	4.57
10	1.08 ± 0.02 (0.999)	6.42	128	−2.00
10 + COD	1.01 ± 0.04 (0.993)	6.86		
11	6.6 ± 0.2 (0.995)	1.1	145	2.73
11 + COD	4.49 ± 0.09 (0.999)	1.54		
12[c]	too fast to measure		170	9.70

[a] Correlation coefficient in parentheses. [b] From ref 52. [c] Complex **12** not isolated due to rapid decomposition, see text.

tetrafluoroborate only, along with signals between 1 and 2 ppm attributed to PCy_3. We conclude that **12** forms initially but decomposes too rapidly to allow isolation of the complex. Thus, it seems that PCy_3 promotes very rapid decomposition. Further qualitative information on the rate effect of different phosphines is obtained from [PdMe(dmiy)(dppp)]BF_4 **13** (dppp = 1,3-bis-(diphenylphosphino)propane).[51] A solution of this complex failed to show any decomposition even after 24 h when monitored by ^{1}H NMR spectroscopy.

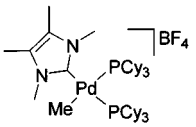

12

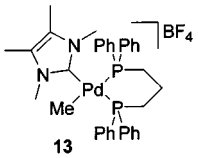

13

Table 1 also lists the steric bulk of the different phosphorus ligands, expressed as the cone angle θ, and the basicity of the ligands, expressed as the pK_a of the conjugate acid,[52] which gives a good measure of the ability of the ligand to donate σ electrons to a metal. It is apparent that the rate of reaction does not correlate well with ligand basicity. The most basic ligand used, PCy_3, results in the fastest decomposition, while the second most basic ligand, $PMePh_2$, gives the slowest rate. If the cone angle of the phosphines is considered, it appears that greater steric bulk favors elimination; however complex **9**, containing the phosphine $PMePh_2$ with a cone angle of 136°, decomposes more slowly than complex **10**, which contains $P(OPh_3)$ with a cone angle of 128°. It is manifest that ligand basicity and steric bulk have opposing influences on the rate of decomposition. Bulky phosphines clearly destabilize the complexes, but the observed slow rate of decomposition of **9** indicates that a strongly donating phosphine can stabilize the complex, providing the steric bulk of the ligand is not too great. The stability of complex **13**, which contains dppp, suggests that chelation strongly retards the reaction. The relatively slow rate of decomposition of the COD complex **8** is consistent with this premise.

The effect of excess ligand on the kinetics was also studied. The rate of decomposition of **10** on the presence of 0.3, 0.5, and 1.7 equiv of excess $P(OPh)_3$ was found to be the same within experimental error. Thus, the rate is unaffected by excess phosphite, and it seems a mechanism involving prior dissociation of a phosphorus ligand in unlikely, vide infra.

Rate constants for the decomposition of **10** at 20, 25, 30, 35, and 40 °C were obtained which gave a linear Arrhenius plot as shown in Figure 1. From this an activation barrier ($\Delta H^{\ddagger}$) of 23.5 ± 1.3 kcal mol^{-1} was calculated along with an entropy of activation ($\Delta S^{\ddagger}$) of 4.3 ± 0.3 kcal mol^{-1} K^{-1}.

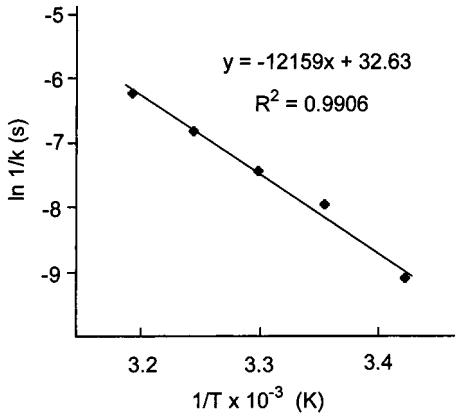

Figure 1. Arrhenius plot for the decomposition of complex **10**.

The kinetics of the reaction could be accounted for by assuming an alkyl migration (path a, Scheme 2), which is followed by rapid further reactions (path d or b,c) to give the products. If this is the case, then migratory insertion must be the rate-determining step, giving a low steady-state concentration of the insertion intermediate—no intermediate in which the methyl group has migrated to the carbene has been observed. Consistent with this idea, β-hydride eliminations are known to be facile, and it is likely that reductive elimination following either path c or d will also be fast.

Insertion reactions (of for example, CO and ethylene) are thought to proceed via opening of the angle between the *cis* nonparticipatory ligands with concomitant closing of the angle between the reacting groups. Chelating ligands can slow the insertion process by locking-in a rigid bite angle.[53−55] The remarkable rate suppression observed when the dppp ligand is bound to Pd is therefore consistent with an insertion process, as is the effect of bulky phosphines, which can cause the angle between the *cis* phosphine ligands to open with a consequent rate increase. However, previous studies into CO and ethylene insertion have shown that migration of the alkyl group is energetically favored by ligands with a high *trans* influence located in the *trans* position to the migrating alkyl group[53] (i.e., the rate of decomposition should increase with strong donor ligands for a mechanism involving alkyl migration). Therefore, in contradiction to the previous arguments, which conform to an insertion process, we find a strong donor ligand stabilizes the carbene complexes to an extent that does not fit a migratory insertion mechanism.

Moreover, aspects of the kinetics are consistent with a concerted reductive elimination (path e, Scheme 2), as first-order rate constants are observed for elimination from dialkyl Pd^{II}, Ni^{II}, and Au^{III} complexes.[47,56−60] For this type of reaction it is known that leaving groups with a strong σ-donor capability favor reductive elimination;[59] hence, the σ-donating ability of heterocyclic carbenes could likewise favor reductive elimination. It has also been noted that positive charge on the metal increases the rate of reductive elimination,[47] which is in agreement with our observations that cationic carbene complexes eliminate

(51) Green, M. J.; Cavell, K. J.; Skelton, B. W.; White, A. H. *J. Organomet. Chem.* **1998**, *554*, 175.
(52) Matiur Rahman, M.; Liu, H.-Y.; Ericks, K.; Prock, A.; Giering, W. P. *Organometallics* **1989**, *8*, 1.
(53) Cavell, K. J. *Coord. Chem. Rev.* **1996**, *155*, 209.
(54) Thorn, D. L.; Hoffmann, R. *J. Am. Chem. Soc.* **1978**, *100*, 2079.
(55) Dekker: G. P. C. M.; Elsevier: C. J.; Vrieze, K.; van Leeuwen, P. W. N. M. *Organometallics* **1992**, *11*, 1598.
(56) Komiya, S.; Albright, T. A.; Hoffmann, R.; Kochi, J. K. *J. Am. Chem. Soc.* **1976**, *98*, 7255.
(57) Tatsumi, K.; Hoffmann, R.; Yamamoto, A.; Stille, J. K. *Bull. Chem. Soc. Jpn.* **1981**, *54*, 1857.
(58) Gillie, A.; Stille, J. K. *J. Am. Chem. Soc.* **1980**, *102*, 4933.
(59) Moravskiy, A.; Stille, J. K. *J. Am. Chem. Soc.* **1981**, *103*, 4182.
(60) Ozawa, F.; Ito, T.; Nakamura, Y.; Yamamoto, A. *Bull. Chem. Soc. Jpn.* **1981**, *54*, 1868.

imidazolium more easily than their neutral counterparts. Coupled with this, and consistent with our observations, is the report that strong σ-donor phosphorus ligands inhibit reductive elimination from PdR_2L_2.[60]

However, for reductive elimination from dialkyl Pd complexes, PdR_2L_2, it has been shown that a dissociative pathway is preferred such that elimination occurs from an intermediate with either a T or Y geometry generated after dissociation of a ligand, L.[57−60] Thus, addition of excess ligand (usually phosphine) severely inhibits reductive elimination. This is in contrast to the decomposition reaction of the present study, which remains unaffected by excess phosphite. Nonetheless, at least one study has shown that reductive elimination from four coordinate PdR_2L_2 is possible when one of the R groups is styryl.[61] It is worth noting in this context that the carbene carbon is sp^2 hybridized with a formally empty but in reality appreciably occupied p-orbital perpendicular to the plane of the carbene (vide infra)[44,45,62] and in this respect it has similarities to a phenyl or alkenyl ligand.[63] Theoretical studies have shown that reductive elimination from four coordinate Pd is possible.[57] The same study showed that reductive elimination from a four-coordinate species is accompanied by an increase in the angle between the two nonparticipatory ligands as the reaction proceeds. This would help account for the rate enhancement afforded by more bulky phosphines, as well as accounting for the strong stabilizing effect that the dppp ligand has on the carbene complex **13**. Furthermore, several theoretical studies[64−66] have shown what is known from experiment,[67−69] that *cis* chelating ligands result in a more exothermic oxidative addition, or stated differently, *a chelating ligand will result in a more endothermic reductive elimination*.

2.3. Theoretical Studies. 2.3.1. Computational Methods. Full geometry optimizations were carried out with the use of the B3LYP[70−72] density functional level of theory combined with two different basis sets: the LANL2DZ basis set (which incorporates the Hay and Wadt[73] small-core relativistic effective core potential and double-ζ valence basis set on palladium and phosphorus together with the Dunning/Huzinaga[74] double-ζ basis set on other atoms), and the DSP basis set (which incorporates the small-core relativistic effective core potential and triple-ζ valence basis set from the Stuttgart group of Dolg, Stoll, Preuss, and co-workers[75] on palladium together with the 6-311G(d,p)[76−78] basis set on other atoms). Sets of five d-functions were used in the basis sets throughout these calculations. For the optimized geometries, harmonic vibrational frequencies were calculated at the B3LYP level and zero-point vibrational energy corrections obtained using unscaled frequencies. The vibrational frequencies were also used to obtain thermodynamic corrections and entropies. All transition structures possessed one and only one imaginary frequency, and they were further characterized by following the corresponding normal mode toward each product and reactant. Single-point energies on B3LYP/LANL2DZ optimized geometries were calculated at the B3LYP level with the LANL2augmented: 6-311+G(2d,p) basis set,[79] which incorporates the LANL2 effective core potential and the large f-polarized valence basis set of Bauschlicher and co-workers[80] on palladium together with the 6-311+G(2d,p) basis set[76−78] on all other atoms. Calculations on the large triphenyl phosphite system were carried out with the ONIOM[81−83] method in which the high layer (at B3LYP/LANL2DZ) employed PH_3 and the low layer (at RHF/LANL2MB) employed $P(OPh)_3$. All calculations were carried out with the Gaussian 98[84] program.

2.3.2. Calculations on a Model System. As the kinetics of the reaction were in part consistent with both a concerted reductive elimination and a multistep insertion process, the reaction was modeled theoretically using $[PdMe(dmiy)(PH_3)_2]^+$ **14** as the model complex, giving 1,2,3-trimethylimidazolium and $Pd(PH_3)_2$ as decomposition products (Reaction 6).

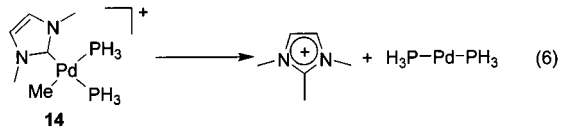

14 (6)

The PES was initially probed for intermediates in both a multistep migratory process and a concerted reductive elimination. We were unable to find a pathway that corresponded to alkyl migration on the PES, however stationary points corresponding to reductive elimination were found. Figure 2 shows the optimized geometries of the reactant **14**, the transition structure **14-15**, the post reductive elimination encounter complex **15**, and the products. In Table 2 the calculated gas-phase bonding parameters of **14** have been compared with the experimental values of some Me−Pd carbene complexes; $PdMeCl(dmiy)_2$,[19] $PdMeCl(tmiy)_2$[85] and $PdMe(dmiy)(NC_5H_4\text{-}CO_2\text{-}2)$.[51] It may be seen that the agreement between experiment

(61) Loar, M. K.; Stille, J. K. *J. Am. Chem. Soc*. **1981**, *103*, 4174.
(62) Heinemann, C.; Müller, T.; Apeloig, Y.; Schwarz, H. *J. Am. Chem. Soc*. **1996**, *118*, 2023.
(63) Low, J. J.; Goddard W. A., I. *J. Am. Chem. Soc*. **1986**, *108*, 6115.
(64) Sakaki, S.; Biswas, B.; Sugimoto, M. *J. Chem. Soc., Dalton Trans*. **1997**, 803.
(65) Sakaki, S.; Biswas, B.; Sugimoto, M. *Organometallics* **1998**, *17*, 7, 1278.
(66) Su, M.-D.; Chu, S.-Y. *Inorg. Chem*. **1998**, *37*, 3400.
(67) Hackett, M.; Ibers, J. A.; Jernakoff, P.; Whitesides, G. M. *J. Am. Chem. Soc*. **1986**, *108*, 8094.
(68) Hackett, M.; Ibers, J. A.; Whitesides, G. M. *J. Am. Chem. Soc*. **1988**, *110*, 1436.
(69) Hackett, M.; Whitesides, G. M. *J. Am. Chem. Soc*. **1988**, *110*, 1449.
(70) Becke, A. D. *J. Chem. Phys*. **1993**, *98*, 5648.
(71) Stephens, P. J.; Devlin, J. F.; Chabalowski, C. F.; Frisch, M. J. *J. Phys. Chem*. **1994**, *98*, 11623.
(72) Hertwig, R. H.; Koch, W. *Chem. Phys. Lett*. **1997**, *268*, 345.
(73) Hay, P. J.; Wadt, W. R. *J. Chem. Phys*. **1985**, *82*, 299.
(74) Dunning, T. H.; Hay, P. J. In *Modern Theoretical Chemistry*; Schaefer, H. F., Ed.; Plenum: New York, 1976; Vol. 3, p 1.
(75) Andrae, D.; Haeussermann, U.; Dolg, M.; Stoll, H.; Preuss, H. *Theor. Chim. Acta* **1990**, *77*, 123.
(76) Krishnan, R.; Binkley, J. S.; Seeger, R.; Pople, J. A. *J. Chem. Phys*. **1980**, *72*, 650.
(77) McLean, A. D.; Chandler, G. S. *J. Chem. Phys*. **1980**, *72*, 5639.
(78) Frisch, M. J.; Pople, J. A.; Binkley, J. S. *J. Chem. Phys*. **1984**, *80*, 3265.
(79) Frankcombe, K. E.; Cavell, K. J.; Yates, B. F.; Knott, R. B. *J. Phys. Chem*. **1996**, *100*, 18363.
(80) Langhoff, S. R.; Petterson, L. G.; Bauschlicher, C. W.; Partridge, H. J. *J. Chem. Phys*. **1987**, *86*, 268.
(81) Maseras, F.; Morokuma, K. *J. Comput. Chem*. **1995**, *16*, 1170.
(82) Svensson, M.; Humbel, S.; Froese, R. D. J.; Matsubura, T.; Sieber, S.; Morokuma, K. *J. Chem. Phys*. **1996**, *100*, 19357.
(83) Dapprich, S.; Komaromi, I.; Byun, K. S.; Morokuma, K.; Frisch, M. J. *J. Mol. Struct. (THEOCHEM)* **1999**, *462*, 1.
(84) Frisch, M. J.; Trucks, G. W.; Schlegel, H. B.; Scuseria, G. E.; Robb, M. A.; Cheeseman, J. R.; Zakrzewski, V. G.; Montgomery, J. A., Jr.; Stratmann, R. E.; Burant, J. C.; Dapprich, S.; Millam, J. M.; Daniels, A. D.; Kudin, K. N.; Strain, M. C.; Farkas, O.; Tomasi, J.; Barone, V.; Cossi, M.; Cammi, R.; Mennucci, B.; Pomelli, C.; Adamo, C.; Clifford, S.; Otcherski, J.; Petersson, G. A.; Ayala, P. J.; Cui, Q.; Morokuma, K.; Malick, D. K.; Rabuk, A. D.; Raghavachari, K.; Foresman, J. B.; Cioslowski, J.; Ortiz, J. V.; Stefanov, B. B.; Liu, G.; Liashenko, A.; Piskorz, P.; Komaromi, I.; Gomberts, R.; Martin, R. L.; Fox, D. J.; Kieth, T.; Al-Laham, M. A.; Peng, C. Y.; Nanayakkara, A.; Gonzalez, C.; Challacombe, M.; Gill, P. M. W.; Johnson, B. G.; Chen, W.; Wong, M. W.; Andres, J. L.; Head-Gordon, M.; Replogle, E. S.; Pople, J. A. *Gaussian 98*, rev. A.1.; Gaussian, Inc: Pittsburgh, PA, 1998.
(85) Magill, A. M.; McGuinness, D. S.; Cavell, K. J.; Britovsek, G. J. P.; Gibson, V. C.; White, A. J. P.; Williams, D. J.; White, A. H.; Skelton, B. W. *J. Organomet. Chem* **2001**, *617−618*, 546.

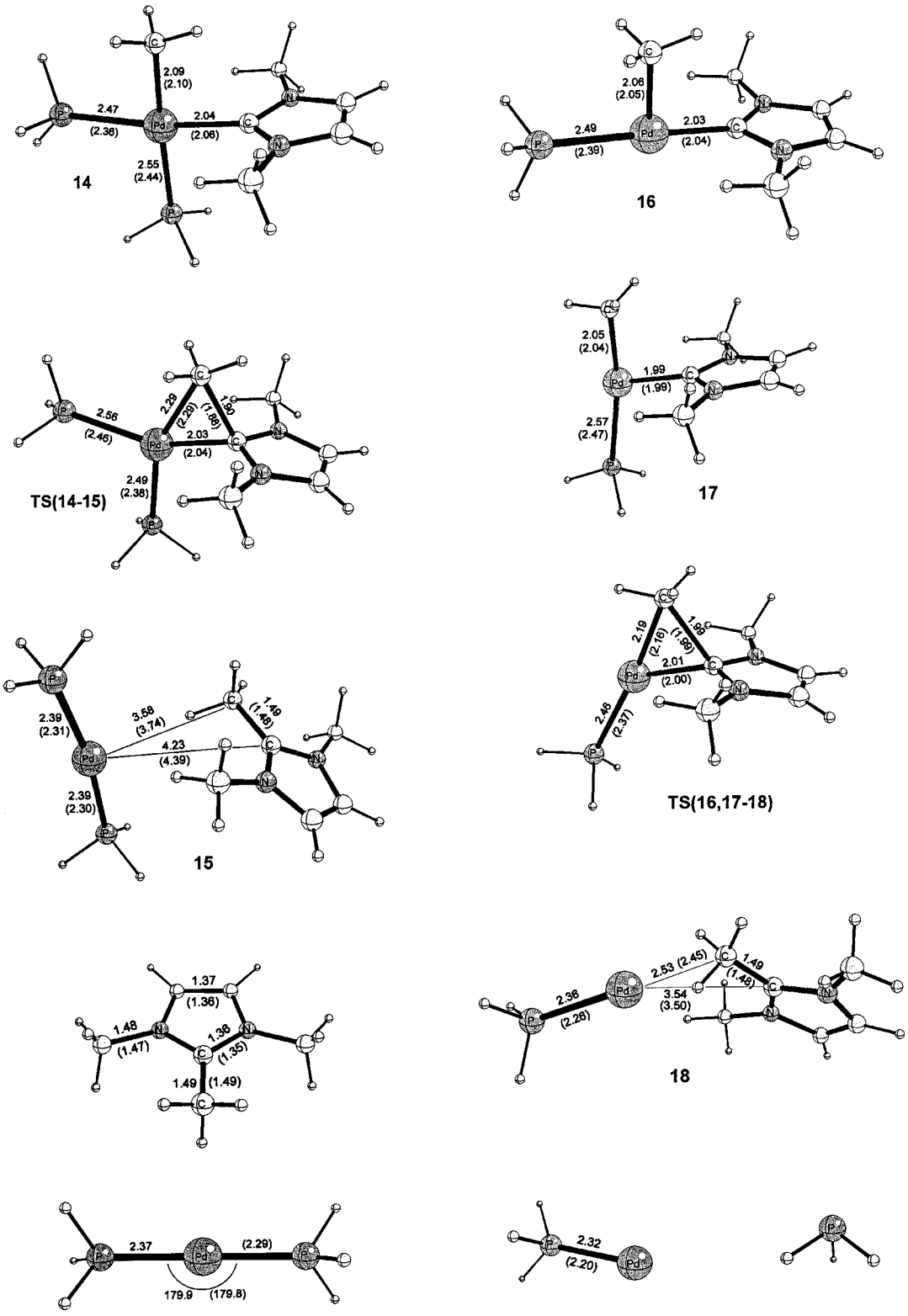

Figure 2. Optimized geometries (B3LYP/LANL2DZ) corresponding to reductive elimination from complex **14** (left) and complexes **16** and **17** (right). Bond lengths are given in Å and angles in degrees, values in parentheses represent B3LYP/DSP optimized geometries.

and theory is in most cases excellent. Furthermore, Table 2 shows that the geometries obtained with both the LANL2DZ and DSP basis sets are almost the same. Table 3 compares the calculated geometry of 1,2,3-trimethylimidazolium with the experimental geometries of 1,2-dimethyl-3-propylimidazolium chloride (dmpim)Cl[86] and pentamethylimidazolium iodide (pmim)I,[87] and again the level of agreement between experiment and theory, and the two basis sets is excellent.

Reductive elimination with prior dissociation of one phosphorus ligand was modeled by removing one phosphine from the complex. The optimized geometries of the stationary points corresponding to this pathway are also shown in Figure 2. Two

(86) Scordilis-Kelly, C.; Robinson, K. D.; Belmore, K. A.; Atwood, J. L.; Carlin, R. T. *J. Crystallogr. Spectrosc. Res.* **1993**, *23*, 601.

(87) Kuhn, N.; Henkel, G.; Kreutzberg, J. *Z. Naturforsch.* **1991**, *46b*, 1706.

Table 2. Comparison of Calculated Bond Lengths (Å) and Bond Angles (deg) in PdMe(dmiy)(PH_3)$_2$ **14** with Experimental Values of Several Me−Pd Carbene Complexes[19,85,51]

parameter	**13** (DSP)[a]	**13** (LANL2DZ)[b]	PdMeCl(dmiy)$_2$	PdMeCl(tmiy)$_2$	PdMe(dmiy) ($NC_5H_4CO_2$−2)
Pd−$C_{carbene}$	2.06	2.04	1.999(7), 2.009(8)	2.033(4)	1.971(2)
N−$C_{carbene}$	1.35	1.38	1.36(1), 1.369(9), 1.345(9)	1.345(5), 1.347(5)	1.347(3), 1.348(3)
N−CH_3	1.46	1.47	1.48(1), 1.46(1), 1.45(1)	1.456(7), 1.472(6)	1.456(4), 1.461(4)
C═C	1.35	1.37	1.33(1), 1.32(1)		1.339(4)
N−C−N	105.2	105.0	102.1(6), 103.2(6)	103.1(3)	104.6(2)
C_c−N−CH_3	125.5	125.2	122.9(7)−123.8(6)	123.7(3), 124.5(3)	124.7(2), 124.0(2)
C_c−N−C	110.6	110.7	111.5(6)−112.5(7)		110.9(2)

[a] B3LYP/DSP optimization. [b] B3LYP/LANL2DZ optimization.

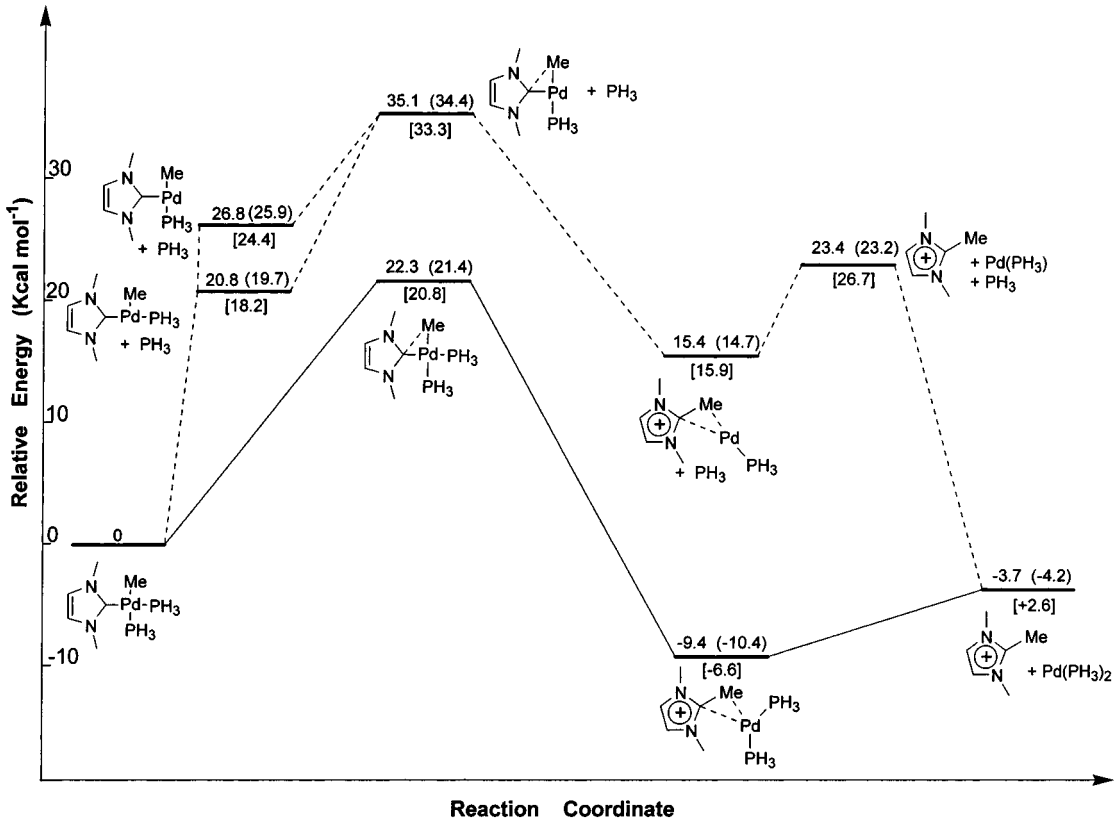

Figure 3. Potential energy profile for reductive elimination from four-coordinate Pd (solid line) and with prior phosphine dissociation (dashed line). Energies are from B3LYP/augmented LANL2DZ:6-311+G(2d,p)//B3LYP/LANL2DZ calculations. Values in parentheses represent B3LYP/DSP energies, and those in brackets, B3LYP/LANL2DZ energies, see text.

Table 3. Comparison of Calculated Bond Lengths (Å) and Bond Angles (deg) in 1,2,3-trimethylimidazolium with Experimental Values of (dmpim)Cl[86] and (tmim)I[87]

parameter	DSP[a]	LANL2DZ[b]	(dmpim)Cl	(tmim)I
C−CH_3	1.48	1.49	1.486(6)	1.48(2)
N−C	1.35	1.36	1.339(5), 1.334(6)	1.32(2), 1.35(2)
N−CH_3	1.47	1.48	1.488(6)	1.47(2), 1.50(2)
C═C	1.36	1.37	1.327(6)	1.38(2)
N−C−N	107.4	107.2	107.1(4)	106.2(11)
C−N−CH_3	125.5	125.6	125.8(4)	124.0(11), 125.8(11)
C−N−C	109.2	109.3	109.4(4)	110.5(10), 112.2(10)

[a] B3LYP/DSP optimization. [b] B3LYP/LANL2DZ optimization.

isomeric starting complexes were found, corresponding to phosphine dissociation *trans* to the methyl group (**16**) and dissociation of the phosphine *trans* to the carbene (**17**). It is expected that there would be a small barrier to interconversion of **16** and **17**, although we did not attempt to find this. Only one transition structure, **TS(16,17-18)**, was found, which leads to the post reductive elimination encounter complex **18**. Presumably complex **16** proceeds to the transition structure through **17**, which is higher in energy (vide infra). Reductive elimination is predicted to occur from a T shaped geometry, which was also predicted by Hoffmann et al. using extended Hückel calculations on PdR_2L.[57]

Figure 3 shows the potential energy profile for the elimination from both complex **14** and the three coordinate complexes **16** and **17**. All energies are relative to the starting complex **14**, and in the case of elimination with phosphine dissociation, the energies given are with free PH_3 added. The energies in parentheses are from B3LYP/DSP calculations and those in brackets represent B3LYP/LANL2DZ energies. Figure 3 shows that the level of agreement is in general quite good, and in further discussion the B3LYP/augmented LANL2DZ:6-311+G(2d,p) energies will be used. Reductive elimination from **14** is predicted to occur with an enthalpy of activation of 22.3 kcal mol^{-1}, which seems very reasonable given the experimental value of 23.5 kcal mol^{-1} for the triphenyl phosphite complex in solution.[88] The reaction is predicted to be slightly exothermic, the products lying 3.7 kcal mol^{-1} below the reactant.

Dissociation of a phosphine not surprisingly, is an endothermic process. It takes 26.8 kcal mol^{-1} for the phosphine *trans*

(88) As noted by a reviewer, the theoretical $\Delta H^{\ddagger}$ and $\Delta S^{\ddagger}$ values are calculated for the gas-phase and do not take into account the solvation effects.

to the carbene to dissociate compared to 20.8 kcal mol^{-1} for that *trans* to the Me group. The methyl group therefore has a higher *trans* effect than the carbene, and this is reflected in the differing Pd−P bond lengths in **14**. The energy required to remove a phosphine makes this pathway higher in energy along the complete potential energy profile, relative to the reaction without prior dissociation. The activation barrier, $\Delta H^{\ddagger}$, for **TS-(16,17-18)** is predicted to be 35.1 kcal mol^{-1}, which is 12.8 kcal mol^{-1} higher than that with two coordinated phosphines, **TS(14-15)**. The encounter complex **18** is similarly higher in energy, this time 24.8 kcal mol^{-1} higher than **15**. It is also interesting to note the much closer approach of the imidazolium ion in **18** compared to **15** which is stabilized by an additional phosphine ligand (Figure 2). The important conclusion from the potential energy profile is that reductive elimination occurs from the four coordinate complex **14**, and that prior dissociation of a phosphine is neither required nor favorable. This outcome is in accord with the kinetic results.

Geometry changes during the reaction include a decrease in the Me−Pd−$C_{carbene}$ angle from 85.7° in **14** to 52.0° in **TS-(14-15)** and a concomitant but smaller increase in the P−Pd−P angle from 95.3° to 98.3°. The Pd−Me distance increases from 2.09 to 2.29 Å while the Pd−$C_{carbene}$ distance barely changes in the transition structure. These changes indicate an early, reactant like transition structure. The Me−$C_{carbene}$ distance in the transition structure is 1.90 Å which decreases to 1.49 Å in the encounter complex, and in the free imidazolium cation. During reductive elimination the P−Pd−P angle increases from that in the transition structure (98.3°) to 166.0° in the encounter complex, and to 179.9° in the product, $Pd(PH_3)_2$. These changes are very similar to those predicted for conventional reductive elimination,[64−66] and indicate that a chelating ligand may well hinder the reaction to an extent, as found experimentally.

2.3.3. Calculations on the Real System. Using PH_3 as spectator ligand in the calculations was useful for expediting the elucidation of possible reaction pathways. However this ligand differs from tertiary phosphines/phosphites both in terms of steric and electronic effects. To verify that the same mechanism is likely when 'real' ligands are coordinated, the energetics of reductive elimination from PdMe(dmiy){$P(OPh)_3$}$_2$ **19** were calculated. The only difference between **19** and the isolated complex **10**, for which activation parameters have been experimentally obtained, is the presence of methyl groups in the C4,5 positions of the carbene, which is not expected to greatly influence the energetics of the reaction.

The optimized geometries of **19**, the transition structure **TS-(19-20)**, the encounter complex **20** and the product, Pd-{$P(OPh)_3$}$_2$ are shown in Figure 4. The increased steric bulk of $P(OPh)_3$ results in an increased P−Pd−P angle (103.5°) in **19** relative to that in complex **14** (95.3°). This is accompanied by a decrease in the Me−Pd−carbene angle (81.9° compared to 85.7°). In the transition structure **TS(19-20)** the P−Pd−P angle increases to 114.1°, an increase of 10.6° from that of the initial complex. This increase is greater than that which occurs in going from **14** to **TS(14-15)**. Despite this, the positions of the Me and carbene groups in the transition structure are very similar in both **TS(14-15)** and **TS(19-20)**. The Pd−Me, Pd−$C_{carbene}$ and Me−$C_{carbene}$ distances in **TS(19-20)** are 2.31, 2.04 and 1.97 Å respectively, compared to distances of 2.29, 2.03 and 1.90 Å in **TS(14-15)**.

A potential energy profile for the reaction is shown in Figure 5. The activation barrier is predicted to be 14.1 kcal mol^{-1}, somewhat lower than the experimental value found for complex **10** (23.5 ± 1.3 kcal mol^{-1}). The theoretical $\Delta S^{\ddagger}$ value of 3.8 cal mol^{-1} K^{-1} compares well with the experimental value of 4.3 ± 0.3 cal mol^{-1} K^{-1}. Compared to the model system, the reaction is predicted to be more exothermic with an enthalpy of reaction of −9.2 kcal mol^{-1}. The differences in geometry between the reactant and transition structure for complexes **14** and **19** demonstrate that the more sterically demanding phosphine ligand, $P(OPh)_3$, results in a greater P−Pd−P angle in both the reactant and transition structure, thus favoring the approach of Me and carbene in the transition structure, and lowering the activation energy as predicted theoretically and found experimentally.

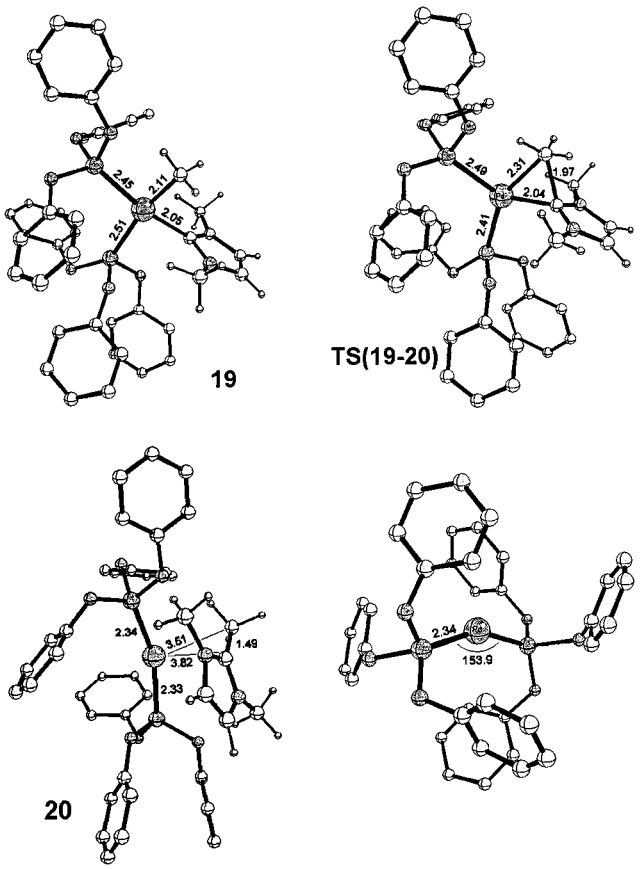

Figure 4. Optimized geometries corresponding to reductive elimination from complex **19**.

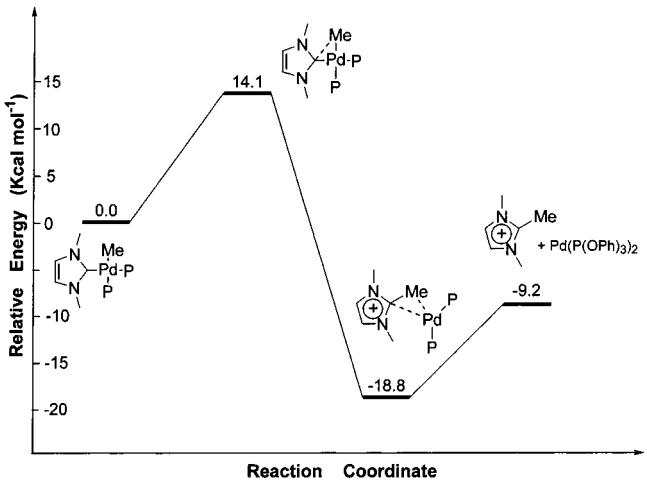

Figure 5. Potential energy profile for reductive elimination from complex **19**.

2.3.4. Bonding in the Reactant, Transition State, and Encounter Complex. The bonding situation in the reactant **14**,

Table 4. Population of the Valence 4d and 5s Orbitals in the Reactant (**14**), the Transition Structure (**TS(14-15)**) and the Product (**15**)

complex	d_{xy}	d_{xz}	d_{yz}	d_{z^2}	$d_{x^2-y^2}$	$\sum d$	s
14	1.92	1.97	1.98	1.95	1.40	9.22	0.52
TS(14−15)	1.88	1.97	1.98	1.95	1.62	9.40	0.43
15	1.90	1.98	1.94	1.96	1.90	9.68	0.61

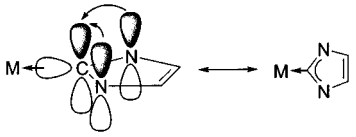

Figure 6.

TS(14-15), and the product **15** was analyzed by the NBO partitioning scheme.[89] Table 4 lists the occupation of the Pd valence 4d and 5s orbitals. The 5p populations are not listed as they were found to be vacant (population < 0.002 in all cases) and are not involved in Pd-ligand bonding. Table 4 shows that the $d_{x^2-y^2}$ orbital in **14** is much less occupied than the other d orbitals, and that the s orbital has a small population. These are the Pd orbitals which are involved in bonding with the ligands, as borne out in the NBO analysis. The methyl group bonds to Pd through interaction of a roughly sp^3 orbital on C with a Pd sd hybrid. Likewise the carbene bonds with Pd through interaction of the expected sp^2 lone pair of carbon with an sd hybrid of Pd. This is shown in Table 5 which contains the occupancy, polarization and hybridization of the Pd−$C_{carbene}$ bond in **14** and **TS(14-15)**.

Previous theoretical and experimental studies by a number of groups have shown that the formally empty p orbital perpendicular to the plane of the carbene ($p(\pi)$) is in fact appreciably occupied due to donation from the $p(\pi)$ lone pairs on the nitrogens.[62,90−92] This N−C π-donation is apparently responsible for the high stability of N-heterocyclic carbenes. It has also been realized that this π-donation is increased on formation of carbene−metal complexes; electron donation from carbene to metal upon complexation is compensated by increased π-donation from the nitrogens. The result is an increase in the population of the C $p(\pi)$ orbital (Figure 6).[44,45] The same situation occurs in complex **14**, and is shown in Table 6, which contains the population, polarization and hybridization of the N−$C_{carbene}$ π bond. The occupation of the $p(\pi)$ NAO on $C_{carbene}$ is 0.83, significantly higher than in the free carbene (0.66).[93] Along with the expected C−N σ bond, there is a bonding orbital between N and $C_{carbene}$ with a population of 1.89. It is purely $p(\pi)$ in character and 25% localized on $C_{carbene}$. This is the N $p(\pi) \rightarrow$ C $p(\pi)$ donation, and results in a low occupation of the N $p(\pi)$ orbitals (1.54).

In the transition structure there is a large increase in the population of the $d_{x^2-y^2}$ orbital, and a similar increase in the total d orbital population, along with a smaller decrease in the s orbital population (Table 4). This observation is consistent with the notion of a reductive elimination. The occupancy of the $C_{carbene}$ $p(\pi)$ orbital has increased somewhat (0.89), but this increase does not come from increased donation from the N $p(\pi)$ orbitals, as the occupancy of the N−C π bond has decreased and is more localized on the nitrogens (Table 6). Furthermore, there is now involvement of a d-function (19.2%) on the carbon side of the N $p(\pi) \rightarrow$ C $p(\pi)$ donor bond, indicating a substantial increase in the polarization of the electron density away from the carbon nucleus. When considering the Pd−$C_{carbene}$ bond, significant d character (41.1%) at the $C_{carbene}$ atom is also found (Table 5). The occupancy of this bond has decreased and is localized more on Pd, which now interacts with $C_{carbene}$ almost purely through d orbitals (97.6%). The Pd s orbital is hardly involved (2.3%) which explains the decrease in the s orbital population. The Pd−C_{Me} NBO has gone in the transition structure and instead a C_{Me}−$C_{carbene}$ bond is found (Table 5). On the C_{Me} side the expected s and p orbitals are involved, while on the $C_{carbene}$ there is also involvement of a d-orbital (23.8%).

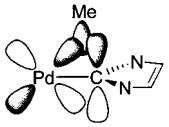

Figure 7.

The above results can be interpreted as follows: in the transition structure there is mixing of the $C_{carbene}$ $p(\pi)$ orbital, the C_{Me} orbital and the Pd d orbitals. This mixing with the $p(\pi)$ and d orbitals allows the $C_{carbene}$−C_{Me} bond to form (Figure 7). Due to the angle of the carbene plane relative to the coordination plane, the $p(\pi)$ orbital, which is directed perpendicular to the carbene plane, is in the correct orientation to interact with the methyl ligand. The increase in the $C_{carbene}$ $p(\pi)$ population is thus explained by its involvement in bonding with C_{Me} in the transition state. The d orbital with the correct orientation for this 3-center interaction is the d_{xy} orbital, and we note a slight decrease in its population in the transition state (Table 4).

Recently Sakaki and co-workers[94] have studied oxidative addition of $(HO)_2B-CH_3$ to $Pd(PH_3)_2$ and have found a similar involvement of the $B(OH)_2$ $p(\pi)$ orbital in the transition state. It should also be noted that there are some similarities between our reaction and reductive coupling of sp^2 phenyl or alkenyl ligands with alkyl ligands. It has been noted that sp^2 hybrids make a less directional bond with the metal than sp^3 hybrids, and therefore more multicentered bonding is possible in the transition structure, which results in lower activation energies for alkyl-alkenyl or alkyl-phenyl coupling.[63] Similar involvement of the $p(\pi)$ orbitals in the transition structures can be envisaged.

Looking at the product, encounter complex **15**, the population of the $d_{x^2-y^2}$ orbital increases further as does the population of the 5s orbital. The $C_{carbene}$−C_{Me} bond is fully occupied and there is no longer any d orbital involvement. The N $p(\pi) \rightarrow$ C $p(\pi)$ is purely p in character as in the reactant complex. The $p(\pi)$ occupancy of the carbon (0.92) has increased due to greater donation for the N $p(\pi)$ orbitals, which is expected from the greater delocalization of the imidazolium cation.

The changes in the partial charges on the ligands and metal are shown in Table 7. The degree of positive charge on the carbene and the methyl ligands increases from start to finish, while the charge on Pd decreases. The changes are thus consistent with the notion of reductive elimination. The total charge on the imidazolium ion (+0.96) and that on $Pd(PH_3)_2$ (+0.04) are very close to those on the separated species, and this indicates that the bonding situation in the encounter complex is very similar to that in the separated species.

2.4. Homogeneous Catalysis with Carbene−Metal Complexes. We have shown above that alkyl-carbene coupling from

(89) Reed, A. E.; Curtiss, L. A.; Weinhold, F. *Chem. Rev.* **1988**, *88*, 899.

(90) Heinemann, C.; Thiel, W. *Chem. Phys. Lett.* **1994**, *217*, 11.

(91) Boehme, C.; Frenking, G. *J. Am. Chem. Soc.* **1996**, *118*, 2039.

(92) Lehmann, J. F.; Urquhart, S. G.; Ennis, L. E.; Hitchcock, A. P.; Hatano, K.; Gupta, S.; Denk, M. K. *Organometallics* **1999**, *18*, 1862.

(93) The NBO analysis of 1,3-dimethylimidazolin-2-ylidene was performed at the B3LYP/6-311+G(2d,p)//B3LYP/LANL2DZ level.

(94) Sakaki, S.; Kai, S.; Sugimoto, M. *Organometallics* **1999**, *18*, 4825.

Table 5. Occupancy, Polarization, and Hybridization of the Pd−$C_{carbene}$ and $C_{carbene}$−Me Bonds in **14**, **TS(14-15)** and **15**

complex	occup	%$C_{carbene}$	%Pd	%s(C)	%p(C)	%d(C)	%s(Pd)	%d(Pd)
				Pd−$C_{carbene}$				
14	1.88	71.9	28.1	38.6	61.4	0	52.4	47.4
TS(14-15)	1.70	13.8	86.2	18.3	40.5	41.1	2.3	97.6
		%$C_{carbene}$	%C_{Me}	%s(C_c)	%p(C_c)	%d(C_c)	%s(C_{Me})	%p(C_{Me})
				$C_{carbene}$−C_{Me}				
TS(14-15)	1.61	42.2	57.8	23.5	52.6	23.8	18.5	81.3
15	1.98	52.8	47.2	40.8	59.2	0	27.3	72.5

Table 6. Occupancy of the $C_{carbene}$ and N p(π) Orbitals, and Occupancy, Polarization, and Hybridization of the N−$C_{carbene}$ p(π) Donor Bond

	p(π) occupancy		N−$C_{carbene}$ p(π) donor bond					
complex	C	N	occup	%C	%N	%p(C)	%d(C)	%p(N)
14	0.83	1.54	1.89	25.0	75.0	99.8	0.2	100.0
TS(14-15)	0.89	1.56	1.79	17.0	83.0	80.5	19.2	99.9
15	0.92	1.48	1.89	27.8	72.2	99.8	0.2	100.0

Table 7. Partial Charges (q) on the Ligands and Metal in **14**, **TS(14-15)**, and **15**

complex	q(carbene)	q(Me)	q($Pd(PH_3)_2$	q(Pd)
14	+0.42	−0.18	+0.76	+0.24
TS(14-15)	+0.46	0.00	+0.54	+0.15
15	+0.86	+0.10	+0.04	−0.31

heterocyclic carbene complexes of Pd can be facile and occurs via a mechanism of concerted reductive elimination. Although not studied in this work, it seems likely that the same mechanism may operate for carbene-hydride, -acyl, and -phenyl couplings on Pd,[20,30,95] and that Ni will also eliminate the imidazolium cation via the same mechanism. Both Pd and Ni−carbene complexes have been applied as catalysts in C−C coupling reactions, so this reaction provides a route by which such catalysts may deactivate. The high activity of Pd−carbene complexes in C−C coupling reactions has been attributed to the high bond dissociation energy of heterocyclic carbenes.[15,17,96] A strongly coordinating ligand will stabilize a catalyst, providing ligand dissociation is the main cause of catalyst decomposition. However, while the bond dissociation may be high, this does not necessarily equate to high catalyst stability, as there are often other low-energy pathways to decomposition not dependent on dissociation. In this paper we have identified such a pathway for catalysts based on hydrocarbyl carbene complexes.

A number of Pd−carbene complexes are among the most active catalysts reported for Heck couplings.[21,85] However, if Pd complexes so readily reductively eliminate, how can this high activity be rationalized? While studying olefin insertion into phenyl−Pd carbene complexes we found that at low temperatures carbene-phenyl reductive coupling predominates, while at higher temperatures insertion and β-hydride elimination effectively competes with reductive coupling.[20] It seems likely that under catalytic conditions (elevated temperature, excess substrate) the insertion/β-hydride elimination steps of the Heck reaction may be faster than reductive elimination, hence the high activity of the catalysts. Our observation that decomposition is observed shortly after the substrates are exhausted is in agreement with the concept of competing pathways.[19] Additional stability would come from anionic coordinating ligands present in solution, and it is also possible that the catalyst resting state is zerovalent, from which reductive coupling cannot occur.

An understanding of the mechanism by which Pd− and Ni−carbene complexes eliminate the imidazolium cation allows us to suggest possible ways in which catalysts may be made more stable, with the anticipation that improved catalytic performance will result. Theoretical results show that for reductive elimination to occur, the carbene and alkyl group must be in a *cis* arrangement, and the angle between them must decrease in the transition structure as they react together. Hence, coordinating functional groups attached to the carbene nitrogens, as in complex **21**, will hinder the necessary *cis* arrangement.

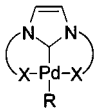

21 X=N,P,O,S

We have recently prepared a number of complexes of this type and have found that when the donor group is suitably coordinating the complex does appear to have higher stability. When weaker donor groups are attached, the complex is much less stable, and the imidazolium cation is readily eliminated.[85] Sterically demanding substituents on the carbene will hinder close approach of the alkyl group and carbene. This is likely to be most effective if the carbene contains out of plane steric bulk, as the carbene interacts with the alkyl group in a side-on manner. Nitrogen substituents such as ^{t}Bu, 2,6-diisopropylphenyl, and adamantyl would achieve this. It is interesting to note that Herrmann et al.[96] found that bulky carbene ligands were important in achieving high activity with mixed carbene-phosphine Pd complexes for Suzuki coupling. Moreover, the approach of the carbene and methyl groups is accompanied by an attendant increase in the angle between the two nonparticipatory ligands in the transition structure. We have shown that fixing this "bite angle" with a chelating diphosphine (complex **13**) slows the decomposition reaction to such an extent that it is not observed at ambient temperature.

2.4.1. Metal-Catalyzed Reactions in Ionic Liquids. A potentially important method to limit decomposition of Pd−carbene complexes, via reductive elimination, is to force the reaction in the reverse direction by operating in a large excess of imidazolium ion—any Pd^0 that forms as a consequence of reductive elimination may re-form the Pd−carbene complex through oxidative addition of the imidazolium ion. To operate in molten imidazolium salt[97] as the solvent would ensure an appropriate excess of ion.

A variety of catalytic reactions have been carried out in ionic liquids, including Ni-catalyzed olefin dimerization[98,99] and Pd-catalyzed Heck reactions.[100−102] One of the most common types of ionic liquids used are those based on substituted imidazolium

(95) In the case of (sp^2) phenyl and acyl coupling with carbenes involvement of the occupied p(π) orbitals is possible.

(96) Weskamp, T.; Böhm, V. P. W.; Herrmann, W. A. *J. Organomet. Chem.* **1999**, *585*, 348.

(97) Welton, T. *Chem. Rev.* **1999**, *99*, 2071.

(98) Chauvin, Y.; Einloft, S.; Olivier, H. *Ind. Eng. Chem. Res.* **1995**, *34*, 1149.

(99) Ellis, B.; Keim, W.; Wasserscheid, P. *J. Chem. Soc., Chem. Commun.* **1999**, 337.

salts,[97] providing an ideal opportunity for reaction between the metal and imidazolium ion. Indeed, in one application of imidazolium salts as solvents for the Heck reaction the possible involvement of Pd−carbene species has been suggested,[100] and in a study on Suzuki coupling reactions with $Pd_2(dba)_3$ as the precatalyst, the apparently successful in situ conversion of imidazolium salt into free carbene has been reported.[22] Very recently, Xiao et al. isolated Pd−carbene complexes from an ionic liquid solvent in which $Pd(OAc)_2$ was used as a precatalyst for the Heck reaction.[102] The formation of carbene complexes in the Heck reaction most likely resulted from deprotonation of the imidazolium C2 proton under the basic conditions of the reaction. However, the apparent formation of Pd−carbene complexes from $Pd_2(dba)_3$ raises the question, can carbene−metal complexes form via an alternative mechanism in which prior deprotonation of the imidazolium cation is not necessary? The present study suggests that they can—through a process of oxidative addition to a low-valent metal. It is known that chelating ligands on zerovalent Pd and Pt favor oxidative addition.[65−69,94] This is a consequence of a bent geometry for the $M^0(L\wedge L)$ fragment, which has a high d-orbital energy relative to linear ML_2. Thus, the reverse reaction (in this case, reductive elimination from a carbene complex containing a chelating ligand) is expected to be disfavored. Consistent with this expectation, our preliminary calculations on the model system PdMe(dmiy)(P∧P) (P∧P = 1,2-diphosphinoethane) show that the reactant is lower in energy than the $Pd^0(P\wedge P)$ and imidazolium products, that is, oxidative addition of imidazolium ion to Pd(P∧P) should be spontaneous. Thus, in principle it is possible to change the energetics of a system to favor oxidative addition to give a carbene complex, especially in a huge excess of imidazolium ion. It is important to note that not only would oxidative addition of an imidazolium ion produce a carbene complex, but it would also generate a reactive metal−hydride that could initiate a catalytic cycle such as dimerization or C−C coupling. Further computational and experimental studies on the oxidative addition reaction[103] and on nickel−carbene catalyzed dimerization reactions will be reported shortly.

3. Conclusions

A number of novel cationic methyl−Pd^{II}−carbene complexes incorporating different phosphine ligands have been prepared and fully characterized. The complexes decompose cleanly to yield methylimidazolium salts as has been observed previously for a variety of Pd and Ni complexes, and this shows that carbene-based catalysts incorporating a hydrocarbyl group in the active species have available a low-energy pathway to decomposition. Combined kinetic and DFT studies show that the mechanism is one of concerted reductive elimination, and not one of carbene insertion into M−R bonds. This new type of reductive elimination suggests there are similarities in the reactivity of M−R bonds and M-heterocyclic carbene bonds, and again highlights the differences between conventional Fischer and Schrock carbenes and N-heterocyclic carbenes. Finally, an understanding of the mechanism by which this reaction occurs has allowed us to postulate methods by which it can be impeded. These methods and the catalysts that result from their application are currently under investigation in our laboratories.

(100) Carmichael, A. J.; Earle, M. J.; Holbrey, J. D.; McCormac, P. B.; Seddon, K. R. *Org. Lett.* **1999**, *1*, 997.

(101) Herrmann, W. A.; Böhm, V. P. W. *J. Organomet. Chem.* **1999**, *572*, 141.

(102) Xu, L.; Chen, W.; Xiao, J. *Organometallics* **2000**, *19*, 1123.

(103) McGuinness, D. S.; Cavell, K. J.; Yates, B. F. *J. Chem. Soc., Chem. Commun.* In press.

4. Experimental Section

4.1. General Comments. All manipulations were carried out using standard Schlenk techniques or in a nitrogen glovebox (Innovative Technology Inc.). All solvents were purified by standard procedures and distilled under nitrogen immediately prior to use. Nuclear magnetic resonance (NMR) spectra were recorded at ambient temperature unless otherwise stated, and peaks are labeled as singlet (s), doublet (d), triplet (t), multiplet (m), and broad (br). Elemental analysis, MS and GC−MS were carried out by the Central Science Laboratory, University of Tasmania. $[PdMeCl(tmiy)]_2$ was prepared as previously described.[19,51]

4.2. Synthesis. [PdMe(tmiy)(COD)]BF_4, 8. A solution of $[PdMeCl(tmiy)]_2$ (71 mg, 0.25 mmol) in 10 mL of DCM was treated with COD (35 μL, 0.29 mmol) and syringed into a suspension of $AgBF_4$ (73 mg, 0.37 mmol) in 3 mL of DCM at −20 °C. The solution was stirred at this temperature for 1 h before being filtered through Celite and the solvent removed in vacuo at −20 °C until ∼2 mL remained. Diethyl ether (4 mL) was added, and the solvent was decanted off the precipitate that formed. After being washing twice with 4 mL of ether the product was dried in vacuo to yield a white powder. Yield: 0.100 g (90%). Anal. Calcd for $C_{16}H_{27}N_2BF_4Pd$: C, 43.61; H, 6.18; N, 6.36. Found: C, 43.62; H, 6.16; N, 6.08. MS (LSIMS) *m*/*z*: 353 $[M]^+$ (100%). ^{1}H NMR (200 MHz, $CDCl_3$, −20 °C): δ 5.79 (s, br, 2H, *H*C═C), 5.66 (s, br, 2H, C═C*H*), 3.75 (s, 6H, NCH_3), 2.68 (m, br, 8H, CH_2), 2.16 (s, 6H, CCH_3), 0.60 (s, 3H, PdCH_3). ^{13}C NMR (50 MHz, $CDCl_3$ $CDCl_3$, −20 °C): δ 165.3 (N*C*N), 126.8 (*C*═$C_{carbene}$), 118.4, 116.2 (*C*═C_{COD}), 35.5 (NCH_3), 29.4, 28.9 (CH_2), 9.2 (H_3CC═CCH_3), 1.7 (PdCH_3).

[PdMe(tmiy)($PMePh_2$)$_2$]BF_4, 9. This complex was prepared in a manner similar to that for **8** using 51.0 mg (0.0.181 mmol) of $[PdMeCl(tmiy)]_2$, 37 mg (0.19 mmol) of $AgBF_4$ and 70 μL (0.37 mmol) of $PMePh_2$. Yield: 0.113 g (85%). Anal. Calcd for $C_{34}H_{41}N_2P_2PdBF_4$: C, 55.72; H, 5.64; N, 3.82. Found: C, 55.07; H, 5.87; N, 3.60. MS (LSIMS) *m*/*z*: 645 $[M]^+$ (30%), 506 $[Pd(PMePh_2)_2]^+$ (10%), 307 $[Pd(PMePh_2)]^+$ (10%), 201 $[PMePh_2]^+$ (100%). ^{1}H NMR (400 MHz, CD_2Cl_2): δ 7.6−7.1 (m, 20H, phenyl*H*), 3.49 (s, 6H, NCH_3), 1.88 (s, 6H, CCH_3), 1.86 (d, *J* = 8 Hz, 3H, PCH_3), 1.45 (d, *J* = 7 Hz, 3H, PCH_3), 0.17 (dd, *J* = 7 Hz, 8 Hz, 3H, PdCH_3). ^{13}C NMR (100 MHz, CD_2Cl_2): δ 132.6 (d, *J* = 11 Hz, phenyl*C*), 131.4 (d, *J* = 12 Hz, phenyl*C*), 130.8 (d, *J* = 2 Hz, phenyl*C*), 130.5 (d, *J* = 2 Hz, phenyl*C*), 129.0 (d, *J* = 10 Hz, phenyl*C*), 128.8 (d, *J* = 9 Hz, phenyl*C*), 126.2 (d, *J* = 3 Hz, *C*═*C*), 35.1 (NCH_3), 13.2 (d, *J* = 27 Hz, PCH_3), 11.9 (d, *J* = 21 Hz, PCH_3), 8.9 (s, H_3CC═CCH_3), −0.27 (d, *J* = 91 Hz, PdCH_3). ^{31}P NMR (162 MHz, CD_2Cl_2): δ 12.3 (d, *J* = 33 Hz), 0.8 (d, *J* = 33 Hz).

[PdMe(tmiy){P(OPh)$_3$}$_2$]BF_4, 10. This complex was prepared in a manner similar to that for **8** using 65.2 mg (0.232 mmol) of $[PdMeCl(tmiy)]_2$, 66 mg (0.34 mmol) of $AgBF_4$, and 125 μL (0.477 mmol) of $P(OPh)_3$. Yield: 0.192 g (87%). Anal. Calcd for $C_{44}H_{45}N_2O_6P_2PdBF_4$: C, 55.45; H, 4.76; N, 2.94. Found: C, 55.51; H, 4.88; N, 3.11. MS (LSIMS) *m*/*z*: 865 $[M]^+$ (3%), 726 $[Pd\{P(OPh)_3\}_2]^+$ (1%), 139 [pentamethylimidazolium]$^+$ (100%). ^{1}H NMR (200 MHz, $CDCl_3$, −20 °C): δ −0.23 (t, *J* = 8.6 Hz, 3H, PdCH_3), 1.88 (s, CCH_3), 2.92 (s, NCH_3), 7.5−7.0 (m, 30H, phenyl*H*). ^{13}C NMR (50 MHz, $CDCl_3$, −20 °C): δ 150.1 (d, *J* = 5 Hz, ipso-phenyl*C*), 149.8 (d, *J* = 8 Hz, ipso*C*), 130.1 (d, *J* = 5 Hz, phenyl*C*), 126.4 (d, *J* = 5 Hz, phenyl*C*), 125.8 (d, *J* = 15 Hz, phenyl*C*), 120.3 (dd, *J* = 6 Hz, 24 Hz, *C*═*C*), 34.4 (NCH_3), 8.7 (H_3CC═CCH_3), 2.7 (d, *J* = 130 Hz, PdCH_3). ^{31}P (162 MHz, CD_2Cl_2, −30 °C): δ 120.3 (d, *J* = 72 Hz), 113.4 (d, *J* = 72 Hz). After some decomposition had occurred signals at 6.7−7.2 ppm appear in the ^{1}H NMR spectrum corresponding to $Pd\{P(OPh)_3\}_2$, along with a singlet at 141.0 ppm in the ^{31}P NMR spectrum.

[PdMe(tmiy)(PPh_3)$_2$]BF_4, 11. This complex was prepared in a manner similar to that for **8** using 52.2 mg (0.186 mmol) of $[PdMeCl(tmiy)]_2$, 44 mg (0.23 mmol) of $AgBF_4$, and 100.4 mg (0.383 mmol) of PPh_3. Yield: 106 mg (67%). HRMS Calcd for $C_{44}H_{45}N_2P_2{}^{104}Pd$: 767.209826. Found: 767.21313. MS (LSIMS) *m*/*z*: 769 $[M]^+$ (7%), 631 [M and MH cluster for $Pd(PPh_3)_2]^+$ (25%), 139 [pentamethylimidazolium]$^+$ (100%). ^{1}H NMR (200 MHz, CD_2Cl_2, −50 °C): δ 7.0−7.5 (m, 30H, phenyl*H*), 3.52 (s, 6H, NCH_3), 1.89 (s, 6H, CCH_3), 0.23 ("t", *J* = 6 Hz, 3H, PdCH_3). ^{31}P NMR (162 MHz, CD_2Cl_2, −30 °C): δ 34.2 (d, *J* = 30 Hz), 21.4 (d, *J* = 30 Hz). After some decomposition has occurred signals at 7.6−7.85 ppm appear in the ^{1}H NMR spectrum

corresponding to $Pd(PPh_3)_2$, along with a singlet at 35.4 ppm in the ^{31}P NMR spectrum.

Acknowledgment. We are indebted to the Australian Research Council for financial support and for providing an Australian Postgraduate Award for D.S.M. We also acknowledge the generosity of Johnson-Matthey for providing a loan of Pd salts. The staff of the Central Science Laboratory (University of Tasmania) are gratefully acknowledged for their assistance in a number of instrumental techniques, and members of the Computational Chemistry group (University of Tasmania) are thanked for their assistance.

Supporting Information Available: Complete kinetic plots for the decomposition of complexes **8**−**11** and optimized geometries and absolute energies of complexes **14**−**20** and 1,3-dimethylimidazolin-2-ylidene (PDF). This material is available free of charge via the Internet at http://pubs/acs.org.

JA003861G